

Supplement of

Responses of surface ozone air quality to anthropogenic nitrogen deposition in the Northern Hemisphere

Yuanhong Zhao, et al.

5 *Correspondence to:* Lin Zhang (zhanglg@pku.edu.cn)

Section S1

The section describes modifications we implemented to the CLM v4.5 model for better simulating the soil NO_x emissions and also reducing the model LAI overestimation. These include addition of soil NO_x emission and NH₃ volatilization processes, and an improved parameterization of nitrogen uptake by plants. We evaluate the CLM simulated results with satellite LAI observations and soil NO_x emissions calculated by GEOS-Chem.

15 S1.1 Soil NO_x emissions

The original CLM4.5 model does not estimate NO_x emissions from soil. Here we implement a process-based parameterization of soil NO_x emission as described by Parton et al. (2001). This parameterization has been recently applied to the land model LM3V-N (Huang et al., 2015). In the parameterization, soil NO_x from nitrification and denitrification is estimated based on the NO_x over N₂O emission ratio, which varies with the gas diffusivity (D/D₀) (Parton et al., 2001).

$$R_{\text{NO}_x:\text{N}_2\text{O}} = 15.2 + \frac{35.4 \times \text{ATAN}\left[0.68 \times \pi \times \left(10 \times \frac{D}{D_0} - 1.86\right)\right]}{\pi} \quad (1)$$

And the gas diffusivity is calculated as a function of air filled porosity (AFPS) (Davidson and Trumbore, 1995):

$$25 \quad \frac{D}{D_0} = 0.209 \times \text{AFPS}^{\frac{4}{3}} \quad (2)$$

Above-soil NO_x emissions are thus derived from soil N₂O emissions as already estimated in CLM4.5 and the $R_{\text{NO}_x:\text{N}_2\text{O}}$ ratios. However, we find that soil NO_x emissions derived from the original CLM and this parameterization show a distinctly

30 different spatial pattern from those calculated in GEOS-Chem with the scheme of
 Hudman et al. (2012) (Figure S1). To improve the consistency, we also add the
 process of NH₃ volatilization and update the parameterization of plant nitrogen uptake
 in the model as described in the sections below. In addition, we have implemented a
 soil temperature (T_{soil}) dependent factor (the equation below) from Xu and Prentice
 35 (2008) to the N₂O and N₂ emission ratio to reduce the CLM high soil NO_x emissions
 at high latitudes.

$$f(T_{\text{soil}}) = \exp\left(308.56 \times \left(\frac{1}{68.02} - \frac{1}{T_{\text{soil}}+46.02}\right)\right) \quad (3)$$

S1.2 NH₃ volatilization

40 NH₃ is highly volatile under high soil temperature and pH conditions. The original
 CLM calculates abnormally high soil NH₄⁺ content over deserts (e.g., more than 20 g
 N m² in Sahara) due to a lack of the NH₃ volatilization process. Here we implement a
 process-based NH₃ volatilization parameterization in CLM following Xu and Prentice
 (2008). NH₃ volatilization from soil (V_{NH_3}) is estimated as a function of water filled
 45 pore space (WFPS), soil pH, and temperature (T_{soil}) given below.

$$V_{\text{NH}_3} = f(\text{pH})f(T_{\text{soil}})(1 - \text{WFPS}) \frac{N_{\text{NH}_4^+}}{b_{\text{NH}_4^+}} \quad (4)$$

where $N_{\text{NH}_4^+}$ is the soil NH₄⁺ content and $b_{\text{NH}_4^+}$ is the buffer parameter for NH₄⁺ (10
 as given by Huang et al. (2015)). The soil pH factor $f(\text{pH})$ and soil temperature
 factor $f(T_{\text{soil}})$ are given below:

$$50 \quad f(\text{pH}) = e^{2 \times (\text{pH} - 10)} \quad (5)$$

$$f(T_{\text{soil}}) = \min\left(1, e^{308.56 \times \left(\frac{1}{71.02} - \frac{1}{T_{\text{soil}}+46.02}\right)}\right) \quad (6)$$

This NH₃ volatilization parameterization corrects the CLM bias in the soil NH₄⁺
 concentration over desert areas, and show consistent results with Xu and Prentice
 (2008).

55

S1.3 Plant nitrogen uptake

In the original CLM4.5, nitrogen uptake by plants is estimated as plant demand as

long as there is sufficient nitrogen supply. However, many factors may influence plant nitrogen uptake, such as soil inorganic nitrogen concentration, the fine root mass, and soil temperature. Here we follow Thomas et al. (2013) and calculate in CLM the plant nitrogen uptake capacity ($U_{n,plant}$) based on the Hanes-wolf mechanism:

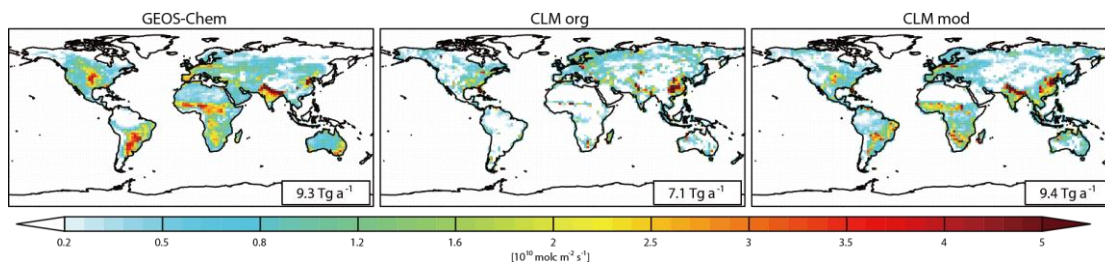
$$U_{n,plant} = V_{n,max} \frac{NH_{4,av} + NO_{3,av}}{(NH_{4,av} + NO_{3,av}) + K_{min}} C_{root} f(T_{soil}) \quad (7)$$

where $V_{n,max} = 2.7 \times 10^{-8} \text{ g N g C}^{-1} \text{ s}^{-1}$ is the maximum N uptake per unit fine root C at 25 °C; $NH_{4,av}$ and $NO_{3,av}$ are available mineral NH_4^+ and NO_3^- in the soil; $K_{min} = 0.83 \text{ g N m}^{-2}$ is the half saturation concentration of fine root nitrogen uptake from Kronzucker et al. (1995; 1996), C_{root} is fine root carbon concentration (g C m^{-2}), and $f(T_{soil})$ represents the limitation of soil temperature on plant nitrogen uptake that we apply the same function as soil decomposition and nitrification in CLM. The calculated uptake capacity is then compared to the plant demand, and the smaller one defines the plant uptake of mineral nitrogen in the modified CLM.

S1.4 Simulated soil NO_x emissions and vegetation LAI

Figure S1 shows the comparison of above-canopy NO_x emissions derived in GEOS-Chem (Hudman et al., 2012) and CLM. We can see that above-canopy NO_x emissions from the modified CLM are in good agreement with the GEOS-Chem results. These modifications also partly correct the significant high biases in CLM simulated LAI relative to satellite measurements from MODIS and AVHRR. As shown in Figure S2, there is about 10% bias reduction in the modified CLM LAI, although large positive biases remain over the Northern Hemisphere continents.

80



85 **Figure S1.** Above-canopy NO_x emissions from soil simulated by GEOS-Chem (left), original CLM (middle), and modified CLM (right). Annual emission totals averaged over 2006-2010 are shown inset.

90

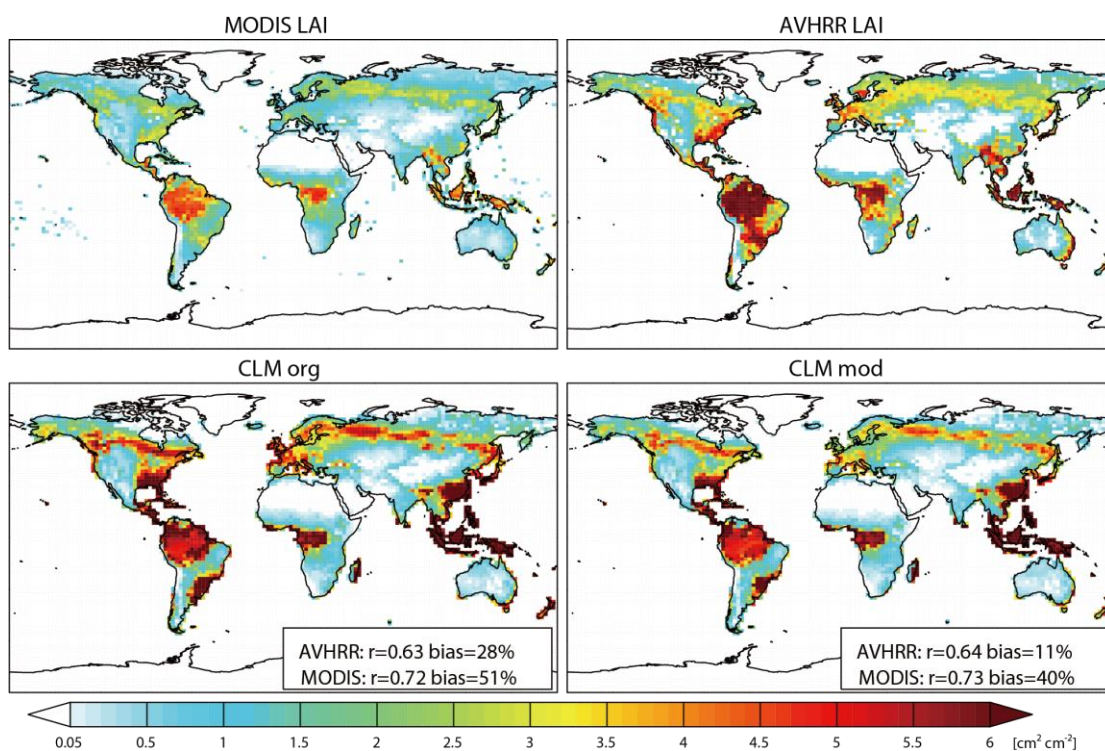
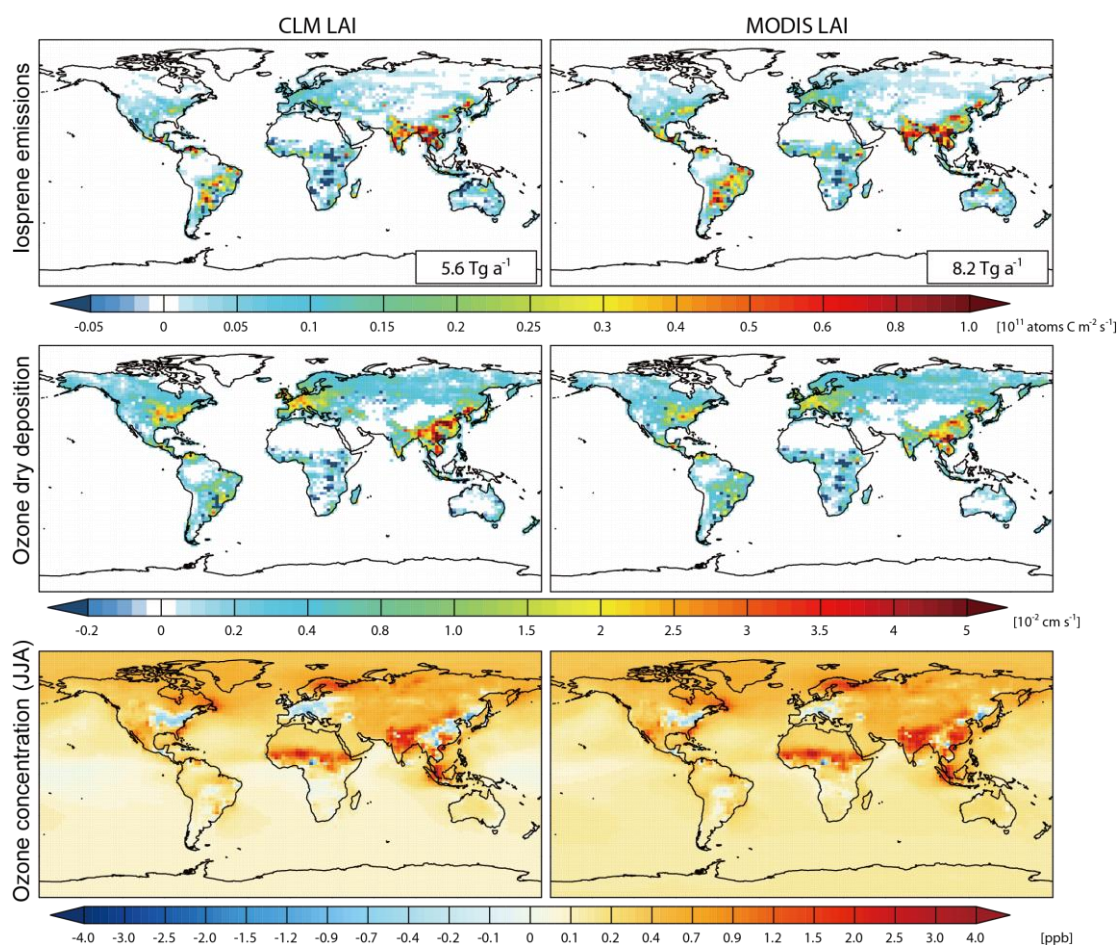


Figure S2. Spatial distribution of annual mean LAI observed from MODIS (top-left panel) and AVHRR (top-right panels) satellite instruments in 2000, as well as those simulated by the original CLM model (CTM org) and our modified model (CLM mod).

95



100

Figure S3. Anthropogenic nitrogen deposition induced changes in biogenic isoprene emissions (top panels, with annual totals shown inset), ozone dry deposition velocity (middle panels), and mean surface ozone concentration for June-July-August (bottom panels) as simulated by GEOS-Chem for 2009. Model results based on the CLM LAI (left panels) are compared to those based on the adjusted MODIS LAI (right panels). The largest differences occur over East Asia and South Asia where the CLM LAI values are distinctly biased high relative to MODIS LAI measurements.

110

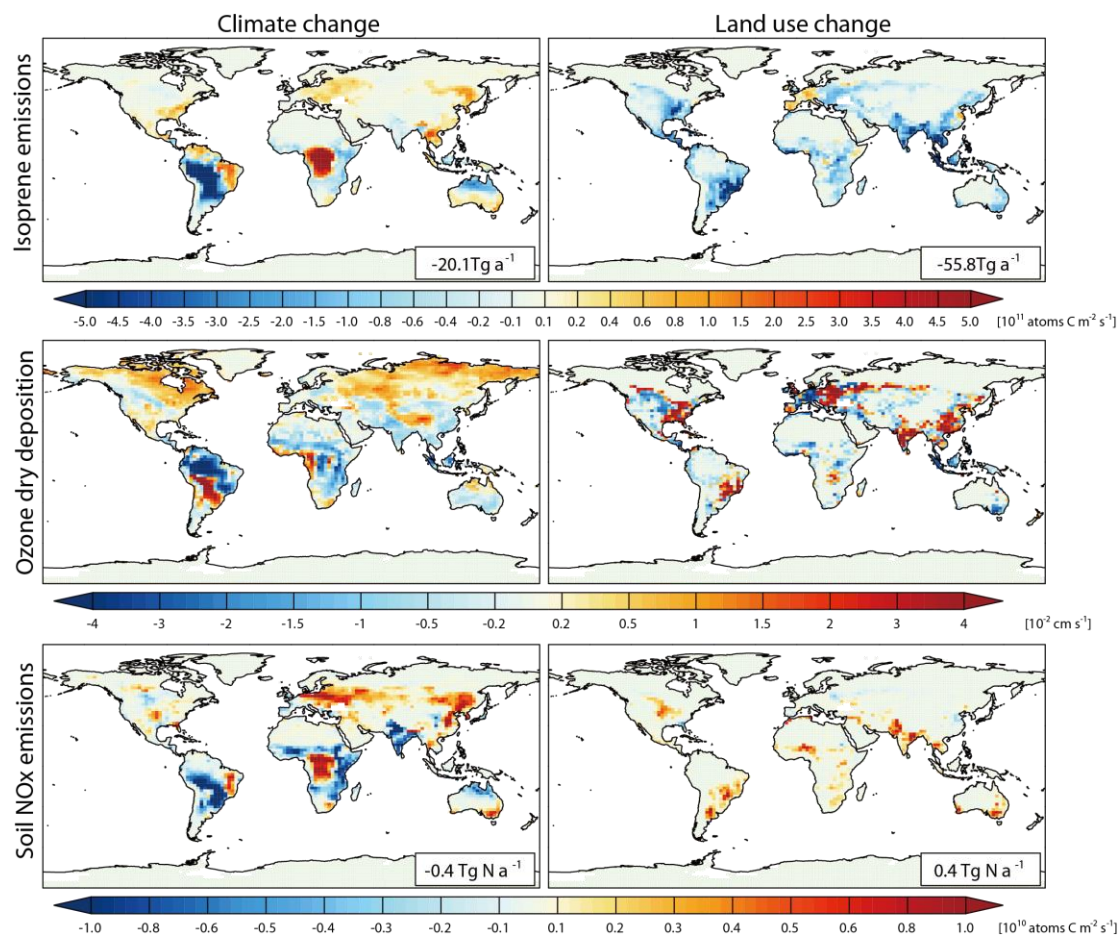


Figure S4. Changes in biogenic isoprene emissions (top panels), ozone dry deposition velocity (middle panels), and soil NO_x emissions (bottom panels) driven by the past 20-year climate change (2006-2010 vs. 1986-1990; left column) and historical land use change (2000 vs. 1860; right column). Annual global emission totals are shown inset.

115

120

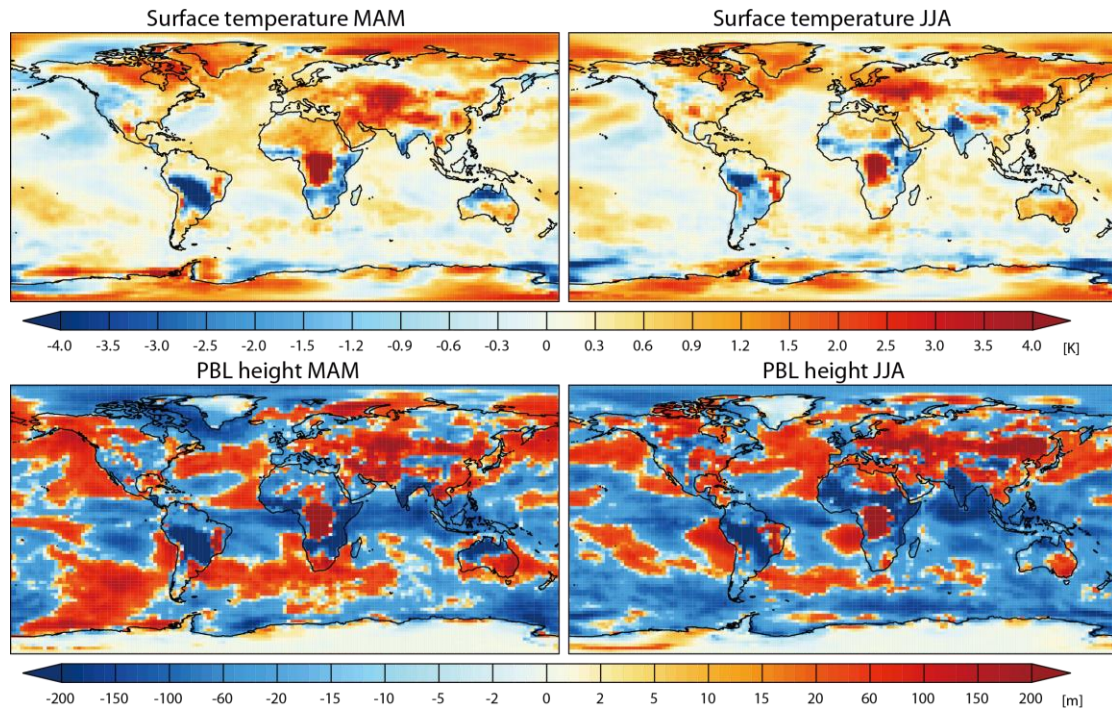


Figure S5. Changes in daytime mean (8:00-18:00 local time) surface temperature (top panels) and planetary boundary height (PBL) (bottom panels) from 1986-1990 to 2006-2010 averaged over March-April-May (left) and Jun-July-August (right).

References

- 130 Davidson, E. A., and Trumbore, S. E.: Gas diffusivity and production of CO₂ in deep soils of the eastern Amazon, *Tellus B*, 47, 550-565, doi: 10.1034/j.1600-0889.47.issue5.3.x, 1995.
- Huang, Y., and Gerber, S.: Global soil nitrous oxide emissions in a dynamic carbon-nitrogen model, *Biogeosciences*, 12, 6405-6427, doi: 10.5194/bg-12-6405-2015, 2015.
- 135
- Hudman, R. C., Moore, N. E., Mebust, A. K., Martin, R. V., Russell, A. R., Valin, L. C., and Cohen, R. C.: Steps towards a mechanistic model of global soil nitric oxide emissions: implementation and space based-constraints, *Atmos. Chem. Phys.*, 12, 7779-7795, doi: 10.5194/acp-12-7779-2012, 2012.
- 140 Kronzucker, H. J., Siddiqi, M. Y., and Glass, A.: Kinetics of NO₃⁻ Influx in Spruce, *Plant Physiology*, 109, 319-326, doi: 10.1104/pp.109.1.319, 1995.
- Kronzucker, H. J., Siddiqi, M. Y., and Glass, A.: Kinetics of NH₄⁺ Influx in Spruce, *Plant Physiology*, 110, 773-779, doi: 10.1104/pp.110.3.773, 1996.
- Parton, W. J., Holland, E. A., Del Grosso, S. J., Hartman, M. D., Martin, R. E., Mosier, A. R., Ojima, D. S., and Schimel, D. S.: Generalized model for NO_x and N₂O emissions from soils, *Journal of Geophysical Research: Atmospheres*, 106, 17403-17419, doi: 10.1029/2001JD900101, 2001.
- 145
- Thomas, R. Q., Bonan, G. B., and Goodale, C. L.: Insights into mechanisms governing forest carbon response to nitrogen deposition: a model–data comparison using observed responses to nitrogen addition, *Biogeosciences*, 10, 3869-3887, doi: 10.5194/bg-10-3869-2013, 2013.
- 150
- Xu, R. I., and Prentice, I. C.: Terrestrial nitrogen cycle simulation with a dynamic global vegetation model, *Global Change Biology*, 14, 1745-1764, doi: 10.1111/j.1365-2486.2008.01625.x, 2008.
- 155